# Real-Time TEM and Kinetic Monte Carlo Studies of the Coalescence of Decahedral Gold Nanoparticles

**Teck H. Lim,[†] David McCarthy,[‡] Shaun C. Hendy,[†,§,*] Kevin J. Stevens,[∥] Simon A. Brown,[‡] and Richard D. Tilley[†]**

[†]MacDiarmid Institute for Advanced Materials and Nanotechnology, School of Chemical and Physical Sciences, Victoria University of Wellington, Wellington, New Zealand, [‡]MacDiarmid Institute for Advanced Materials and Nanotechnology, Department of Physics and Astronomy, University of Canterbury, Christchurch, New Zealand, [§]Industrial Research Ltd., P.O. Box 31-310, Lower Hutt, New Zealand, and [∥]Quest Reliability Ltd., P.O. Box 38-096, Lower Hutt, New Zealand

**ABSTRACT** We report on a real-time *in situ* TEM study of the coalescence of individual pairs of decahedral gold nanoparticles, which have been synthesized in solution. We observe the rate of growth of the neck that joins two particles during coalescence and compare this to classical continuum theory and to atomistic kinetic Monte Carlo simulations. We find good agreement between the observations and the simulations but not with the classical continuum model. This disagreement is attributed to the faceted nature of the particles.

**KEYWORDS:** nanoparticles · coalescence · kinetic Monte Carlo · transmission electron microscopy

The rate of aggregation and coalescence of metal nanostructures are key determinants of their stability and robustness both in and out of the laboratory.[1−3] Once in contact, a pair of nanoparticles will coalesce in order to reduce their surface energy, as confirmed by *in situ* observations,[4−6] and by molecular dynamics simulations.[7−10] Typically, the particles will rapidly form a neck, followed by slower neck growth, and then eventual relaxation to a spherical shape.[4] Below the melting temperature, surface diffusion is expected to be the dominant mass transport mechanism for the coalescence of nanoparticles[11] and thus surface processes will control the time scale for coalescence. While the continuum theory of surface diffusion[11−13] makes predictions about the rate of the coalescence process and its dependence on temperature and particle size, it is not clear that the classical continuum models, which assume isotropic surface tension and surface diffusion constants, are valid for faceted nanostructures below the roughening transition.[14]

More recently, surface diffusion on faceted nanoparticles has been investigated by kinetic Monte Carlo (KMC) methods.[14−16] Combe *et al.*[14,15] used KMC to study the relaxation of face-centered cubic (fcc) nanocrystallites as a function of size and temperature. Below the roughening temperature, they found that relaxation was governed by the time scale for nucleation of new islands on a facet. This time scale depends on the barriers for nucleation of new islands, which in turn depends on the particular crystal facets present. As yet, the relevance of these ideas to nanoparticle coalescence has not been tested, but it is evident from these early studies that the faceted structure and relative orientation of the particles will be important at temperatures well below the particle melting point.

In this article, we report on a real-time *in situ* TEM study of the coalescence of individual pairs of decahedral gold nanoparticles, which have been synthesized in solution.[17] We observe the rate of growth of the neck that joins two particles during coalescence and make comparison with both continuum theory and atomistic KMC simulations. We find good agreement between the observations and the simulations but not with the classical continuum model. We attribute the differences between the experiment and the continuum model to the faceted nature of the particles.

## RESULTS

We focus on the coalescence of two adjacent gold particles initially separated by a distance of ~15 Å. Figure 1a shows the gold nanoparticles as spheres at low magnification. The nanoparticles are nearly monodisperse with an average diameter measured to be 9.5 ± 0.5 nm. Spatially isolated pairs of the nanoparticles could be easily identified as those marked with circles in Figure 1a. The pairs have an average interparticle

*Address correspondence to s.hendy@irl.cri.nz.

Received for review September 14, 2009 and accepted October 20, 2009.

**Published online October 26, 2009.** 10.1021/nn9012252 CCC: $40.75

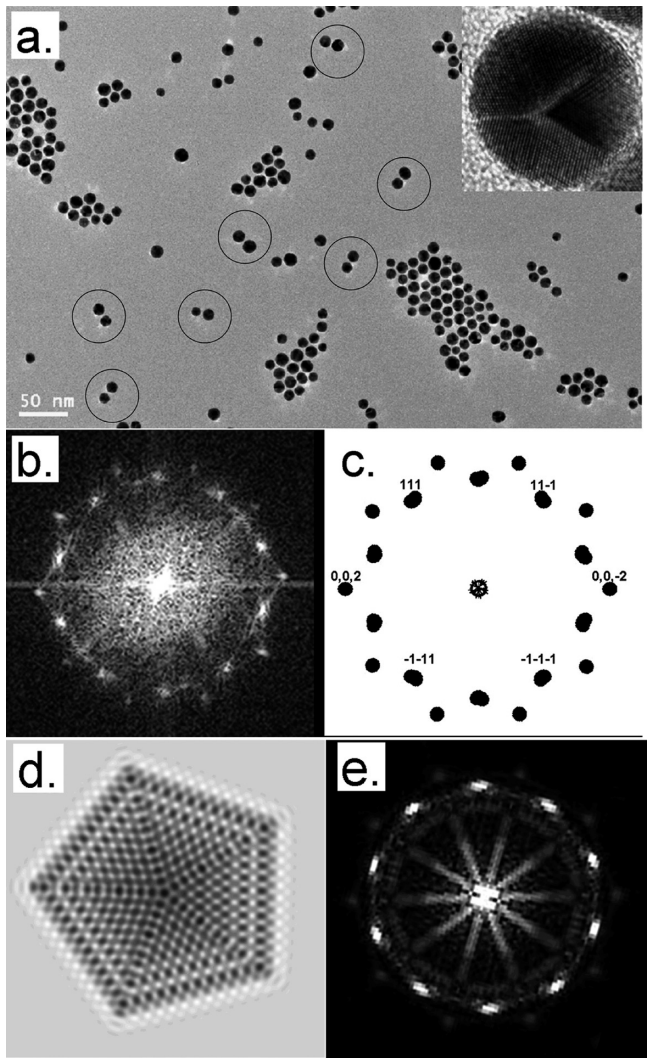


**Figure 1. (a) Low-magnification TEM image of a group of gold decahedral nanoparticles deposited on an amorphous carbon substrate (a TEM grid). The inset shows a typical decahedral nanoparticle in detail at high resolution; (b) power spectrum calculated from the FFT transformation of the inset image; (c) simulated electron diffraction pattern of a decahedral gold crystal viewed down the [110] direction. The diffraction pattern is a superimposition of five fcc gold diffraction patterns. The five diffraction patterns were generated, starting with five identical electron diffraction patterns of a fcc gold crystal viewed down the [110] direction. Rotating four of the five in a sequence of 72, 144, 216, 288°, relative to that at 0° (or 360°) gives the five diffraction patterns to be superimposed; (d) simulated HRTEM image of a gold decahedron model viewed down [110] and (e) the power spectrum calculated from image (d).**

distance of ~15 Å. The interparticle spacing of 15 Å is in good agreement with a 16 Å spacing reported for dodecanethiol-capped silver nanoparticles packed in a hexagonal 2D array.[18]

At high magnification, the nanoparticles can be seen to be decahedral in shape. The inset in Figure 1a shows a typical decahedral gold nanoparticle with five-fold symmetry of the twin boundaries clearly visible. The occurrence of decahedral nanocrystals of gold and silver with five-fold twins is well-documented in the literature, as both metals have low twinning energies and low surface energy anisotropy.[19−23]

The power spectrum (power spectrum 1, Figure 1b) obtained from the Fourier transform (FT) of the high-resolution image is shown as an inset in Figure 1a. To interpret the power spectrum, we compare it first to the diffraction pattern constructed by superposition of five identical single-crystal diffraction patterns of fcc gold viewed down the [110] direction, rotated by 0, 72, 144, 216, and 288°.[20] The rather complicated power spectrum (Figure 1b) is well-matched to the simulated diffraction pattern (Figure 1c). We have also simulated a HRTEM image (Figure 1d) of a model gold Marks decahedron consisting of 4570 atoms viewed down the [110] direction.[24] The FT of this image gives the power spectrum 2 (Figure 1e), which is related to the expected electron diffraction pattern of the model decahedron. An excellent match is found between power spectrum 1 and 2, again confirming that the particles observed are decahedral in shape. In this study, we have examined pairs of gold particles identified to be decahedra.

The coalescence of individual pairs of decahedral gold nanoparticles was recorded *in situ* as videos. To study the coalescence process in detail, still picture frames were extracted from the videos and arranged in sequence according to time chronologically. Figure 2 is a collection of such images which depicts the real-time coalescence process of a pair of decahedral gold nanoparticles intersecting at (100) lattice planes. Starting at an interparticle spacing of ~15 Å, typically ~4−5 min after exposure to an electron beam, coalescence of the nanoparticles commences. The distance between two adjacent particles shortens significantly from 15 to ~2 Å (Figure 2a, already at ~2 Å). The reduction in interparticle spacing is likely due to the loss of oleylamine surfactant, which initially stabilizes the two particles against aggregation. The loss of the surfactant, however, could not be directly observed in the TEM since the size of the surfactant is below the instrumental resolution. In the case of PbSe nanoparticles, van Huis and co-workers have reported the removal of surfactants prior to particle coalescence.[25] When they replaced oleic acid with hexylamine, which has a lower boiling point than that of oleic acid, the coalescence of PbSe is found to occur significantly faster and at a lower temperature than it would be in the case of oleic acid capped particles.

Figure 2b shows the first two "lines" of atoms joining to form the initial physical interface, and as a result, a neck takes form. Accompanying the neck formation is the generation of new surfaces at the periphery of the neck. The surfaces around the initially generated neck are of high degree of curvature (Figure 2b,c). In Figure 2, the neck is marked by two arrows at the neck's apexes, and the distance between the two arrows is the neck diameter. By measuring the neck diameters observed in the picture frames, the neck growth process as a function of time could be monitored and the growth rate quantified.

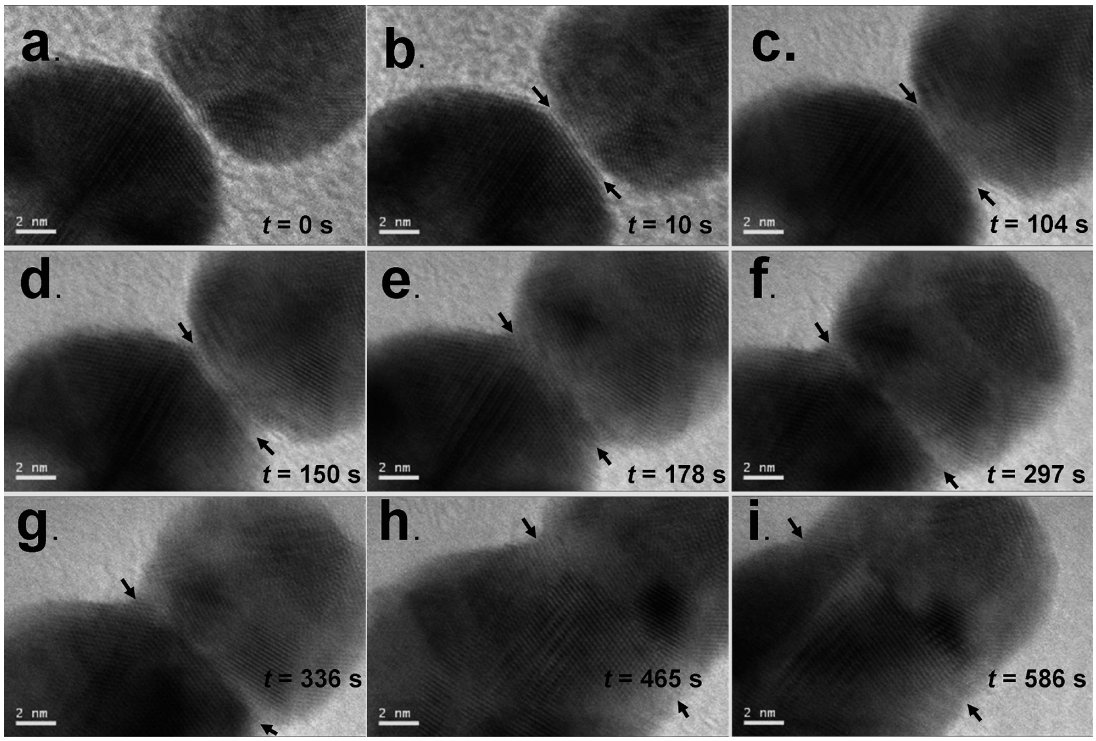


**Figure 2. Time sequence of images captured during *in situ* TEM coalescence of two gold decahedral nanoparticles intersecting at (100) lattice planes. Arrows indicate the apexes of the neck, and the distance between the two arrows is a measure of the neck diameter. The neck diameter increases during the neck growth and the curvature of the surfaces being generated as the neck growth reduces in magnitude continuously and eventually reaches a plateau as shown from (b) to (i).**

The first obvious change is observed at 104 s when the neck becomes more apparent in the image (Figure 2c). During the neck growth, the contrast of the neck becomes darker over time as more gold atoms make up the growing neck. As time passes, the neck diameter increases (Figure 2b−h), until eventually a plateau in neck growth is reached and the two particles form a rod-like oblong shape (Figure 2i).

Throughout the whole coalescence process, lattice fringes and atoms could be clearly identified around the neck region, indicating the absence of a liquid phase. The coalescence therefore proceeds without the nanoparticles melting.[10] Among the several possible mechanisms for particle coalescence without melting, inclusive of hydrodynamic flow, evaporation−condensation, and volume diffusion, surface diffusion is expected to be the dominant mass transport mechanism in small particles.[11] Surface atoms are expected to diffuse from regions of negative curvature into regions of positive curvature (highly curved as near the neck in Figure 2). For a pair of spherical particles coalescing *via* surface diffusion, the neck diameter, $D$, is often observed to grow as a function of time in the form $D \sim t^a$, in which the exponent, $a$, quantifies the order of the power law of the change of neck radius.[11] Classical continuum theory predicts that the values of this exponent should be in the range $a = 1/6-1/7$.[13,14]

To investigate and quantify the rate of the coalescence process, we traced the neck growth as a function of time. In Figure 3, the results of the two sets of observations of neck growth are plotted on log−log axes as the neck grows (note that observation 2 corresponds to the images shown in Figure 2). From Figure 3, the exponent, $a$, for the late-stage neck growth process observed in the experiment was found to be 0.31 in one case (observation 1) and 0.37 in the other (observation 2). These are both considerably larger than that expected from the classical continuum theory of surface diffusion ($a = 1/6-1/7$). Note that in the larger pair of particles (observation 2 as shown in Figure 2) we observed an early-stage neck growth exponent of 0.95 between 100 and 200 s.

To gain further insight into the neck growth process, we performed lattice KMC simulations of the coalescence of a pair of faceted nanoparticles. Our goal was to compare the general form of the neck growth process in the experimental and simulated systems. Therefore, we were less concerned about matching the time scales of the simulated coalescence process to that of the experimentally observed process. Indeed, this would be a difficult and not very informative exercise, as the gold particles are contaminated by oleylamine and will be heated by the electron beam. The coalescence process will also be sensitive to the initial conditions. For instance, the amount of contact between the particles before coalescence begins, the temperature, and the particle size all affect the coalescence and, therefore, the rate at which the neck diameter changes.[16] Hence, we have chosen simulation param-

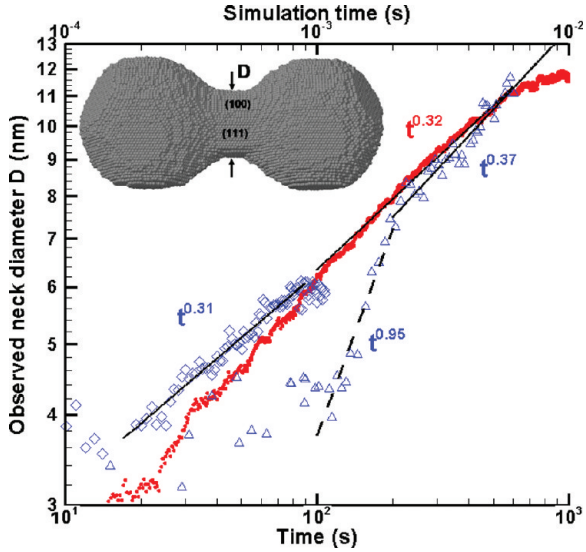


**Figure 3. Evolution of the neck diameter with time (the experimental data are shown by blue, open symbols: observation 1 on diamonds, observation 2 in triangles, while the simulation data are in red solid dots) on a log−log scale. Note that the simulated time scale is shown on the upper horizontal axis while the experimental time scale is on the lower horizontal axis. A power law fit shows the experimentally observed late-stage neck growth process has an exponent, *a*, equal to 0.31 (observation 1) and 0.37 (observation 2), while the simulated process has an exponent of 0.32.**

eters that allow us to compare the general form of the neck diameter's progression to the observations from the experiments rather than precisely match the time scale. It is also difficult to implement lattice KMC for noncrystalline decahedral particles, so single-crystal fcc particles were used. The two particles were oriented so that they met at a (110) plane; this was chosen as it was thought to match best with the experimental situation, where both (100) and (111) facets meet at the neck between the two truncated decahedra. We note that the results of coalescence simulations for other neck orientations have been presented by us elsewhere.[16]

In the simulations, the neck is defined as shown in the inset of Figure 3. The surface of the neck is composed of (111) and (100) facets (see inset). Fitting a power law to the data from $D = 6$ nm to $D = 11$ nm, an exponent $a = 0.32$ is identified. As coalescence proceeds, the (100) facets "grow out" until the particle attains a highly faceted morphology (at $10^{-2}$ s), dominated by large (111) facets. Any further reduction of the particle's surface area requires the nucleation of new layers on (111) facets, which occurs slowly at $T = 500$ K; therefore, after $10^{-2}$ s, the neck diameter changes slowly. It is likely that a similar process has occurred in the experiments, where the particles relax to an oblong rod-like shape rather than to a spherical shape. Previous theoretical studies[8,14] have shown that faceted particles with nonequilibrium shapes can be kinetically stabilized due to the difficulty of nucleating new layers on bare facets. In the classical diffusion model,[11−13] the rate at which material enters the neck changes continuously as the curvature changes. For faceted particles, the rate at which material transfers from the extremities into the neck region changes discontinuously since the ability of the neck to capture diffusing material is dependent on parameters that change discontinuously, for instance, the size, composition, and roughness of the facets at the neck. This discontinuity will act to delay changes in the neck diameter, shifting the increase in neck diameter from the region of the abscissa scale expected by classical diffusion to a later period, which consequently affects the exponent *a* read from the graph.

## SUMMARY

In summary, oleylamine-capped monodisperse decahedral gold nanoparticles of ~10 nm were observed to coalescence *in situ* in a TEM upon exposure to an electron beam. The study presented here combines real-time TEM observations and KMC simulations of the kinetics of the neck growth process, which has not been reported before. Observations of spatially isolated pairs of nanoparticles have revealed a late-stage neck growth process with characteristic power laws of $D \sim t^{0.31-0.37}$, which differ substantially from the relationship $D \sim t^{0.16}$ predicted by the classical continuum theory.[11−13] Likewise, a KMC simulation of the coalescence process using a model of two spherical fcc particles intersecting at (100) facets gave a power law for neck growth of $D \sim t^{0.32}$, which agrees well with the observed experimental power laws, and is due to the particular facets that meet at the neck. This illustrates the crucial role that the faceted structure of nanoparticles plays in their stability to agglomeration and coalescence. Further experimental studies are needed to elucidate the dependence of the coalescence time scales on temperature and particle size, which will be important in developing a good understanding of the stability of metallic nanostuctures.

## METHODS

Decahedral gold nanoparticles were synthesized by modifying the method outlined by Lu and co-workers.[17] Briefly, an oleylamine−AuCl complex was decomposed in toluene under a reducing atmosphere over 2 days at 100 °C. After purification, the gold decahedral nanoparticles were suspended in toluene to form a stable red solution. The oleylamine-capped decahedral gold nanoparticles were then deposited on an amorphous hydrophobic carbon substrate (a TEM grid) by a drop-casting method followed by solvent evaporation. The gold nanoparticles have a strong propensity to form a two-dimensional hexagonal array. By drying a drop (100 μL) of a diluted toluene solution (<2.2 mg/ mL) within 1 min, a TEM specimen with a large number of spatially isolated pairs of gold nanoparticles could be prepared (Figure 1a). This allows us to study the coalescence of two nanoparticles without the interference of others.

A JEOL 2011 TEM with a $LaB_6$ electron source operating at 200 kV was used for TEM and HRTEM analysis. The TEM is equipped with an 11 megapixel Gatan ORIUS SC1000 TEM CCD camera capable of high speed (>14 frames per second) image viewing. When operated in the high speed viewing mode, live images are output as a digital video stream, which was then recorded.

In the TEM, the gold nanoparticles and the oleylamine surfactant residing on the particle surface were impinged by an electron beam, and the coalescence of the nanoparticles would initiate typically within 5 min after their exposure to the electron beam. The coalescence process was viewed at a magnification of 1.2 million times, allowing it to be followed with atomic resolution. During the recording, continuous adjustment of image focus is required due to thermally induced vibration of the TEM sample in the vertical direction parallel to the electron beam. The diameter of the neck during the coalescence was estimated by counting pixels frame by frame in the recorded movie files.

The simulations evolve using hopping rates for atoms which are obtained from a bond counting model. In this model, which has been applied frequently to simulate surface diffusion on fcc crystals,[14−16] the number of initial neighbors, $i$, determines the hopping rate of each atom, the configuration after the jump having no influence on the diffusion. The rate $r_i$ at which an atom with $i$ neighbors will move is $r_i = v \exp(-E_A/k_BT)$, where $v$ is an atomic vibrational frequency (taken here to be $10^{13}$ $s^{-1}$), $T$ the temperature (taken here to be 500 K), and $E_A$ is the activation energy. In the bond counting model, the activation energy is given by $E_A = iE_0$, where $E_0$ is the energy of a single bond. Here we take $E_0 = 0.1$ eV, which is comparable to values found from molecular dynamics simulations of gold nanoparticles.[16] Atoms with many neighbors therefore have small hopping rates and diffuse slowly, while atoms with few neighbors diffuse quickly. The net effect is to shift atoms from regions of negative curvature (*i.e.*, high chemical potential) to regions of positive curvature (lower chemical potential). This results in the growth of the neck when two nanoparticles come into contact.

*Acknowledgment.* We thank the Royal Society of New Zealand for funding through Marsden Fund Contract IRL06004, and the MacDiarmid Institute for Advanced Materials and Nanotechnology for additional funding and experimental facilities.

## REFERENCES AND NOTES

1. Jensen, P. Growth of Nanostructures by Cluster Deposition: Experiments and Simple Models. *Rev. Mod. Phys.* **1999**, *71*, 1695–1735.
2. Baletto, F.; Ferrando, R. Structural Properties of Nanoclusters: Energetic, Thermodynamic, And Kinetic Effects. *Rev. Mod. Phys.* **2005**, *77*, 371–423.
3. Zheng, H.; Smith, R. K.; Jun, Y.-w.; Kisielowski, C.; Dahmen, U.; Alivisatos, A. P. Observation of Single Colloidal Platinum Nanocrystal Growth Trajectories. *Science* **2009**, *324*, 1309–1312.
4. Bonevich, J. E.; Marks, L. D. the Sintering Behavior of Ultrafine Alumina Particles. *J. Mater. Res.* **1992**, *7*, 1489–1500.
5. Palasantzas, G.; Vystavel, T.; Koch, S. A. Coalescence Aspects of Cobalt Nanoparticles during *In Situ* High-Temperature Annealing. *J. Appl. Phys.* **2006**, *99*, 024307.
6. Dai, Z. R.; Sun, S.; Wang, Z. L. Phase Transformation, Coalescence, and Twinning of Monodisperse FePt Nanocrystals. *Nano Lett.* **2001**, *1*, 443–447.
7. Zhu, H.; Averback, R. S. Sintering Processes of Two Nanoparticles: A Study by Molecular-Dynamics Simulations. *Philos. Mag. Lett.* **1996**, *73*, 27–33.
8. Lewis, L. J.; Jensen, P.; Barrat, J. L. Melting, Freezing and Coalescence of Gold Nanoclusters. *Phys. Rev. B* **1997**, *56*, 2248–2257.
9. Zachariah, M. R.; Carrier, M. J. Molecular Dynamics Computation of Nanoparticle Sintering: Comparison with Phenomenological Models. *J. Aerosol Sci.* **1999**, *30*, 1139–1151.
10. Hendy, S.; Brown, S. A.; Hyslop, M. Coalescence of Nanoscale Metal Clusters: Molecular-Dynamics Study. *Phys. Rev. B* **2003**, *68*, 241403.
11. Mullins, W. Theory of Thermal Grooving. *J. Appl. Phys.* **1957**, *28*, 333–339.
12. Nichols, F.; Mullins, W. Morphological Changes of a Surface of Revolution Due to Capillarity-Induced Surface Diffusion. *J. Appl. Phys.* **1965**, *36*, 1826–1835.
13. Kuczynski, G. Study of the Sintering of Glass. *J. Appl. Phys.* **1949**, *20*, 1160–1163.
14. Combe, N.; Jensen, P.; Pimpinelli, A. Changing Shapes in the Nanoworld. *Phys. Rev. Lett.* **2000**, *85*, 110–113.
15. Jensen, P.; Combe, N. Understanding the growth of nanocluster films. *Comput. Mater. Sci.* **2002**, *24*, 78.
16. McCarthy, D.; Brown, S. A. Evolution of neck radius and relaxation of coalescing nanoparticles. *Phys. Rev. B* **2009**, *80*, 064107.
17. Baletto, F.; Mottet, C.; Ferrando, R. Molecular Dynamics Simulations of Surface Diffusion and Growth on Silver and Gold Clusters. *Surf. Sci.* **2000**, *446*, 31–45.
18. Lu, X.; Tuan, H.; Korgel, B.; Xia, Y. Facile Synthesis of Gold Nanoparticles with Narrow Size Distribution by Using AuCl or AuBr as the Precursor. *Chem.—Eur. J.* **2008**, *14*, 1584–1591.
19. Petrova, H.; Juste, J.; Pastoriza-Santos, I.; Hartland, G. V.; Liz-Marzán, L. M.; Mulvaney, P. On the Temperature Stability of Gold Nanorods: Comparison between Thermal and Ultrafast Laser-Induced Heating. *Phys. Chem. Chem. Phys.* **2006**, *8*, 814–821.
20. Elechiguerra, J. L.; Reyes-Gasga, J.; Yacaman, M. J. The Role of Twinning in Shape Evolution of Anisotropic Noble Metal Nanostructures. *J. Mater. Chem.* **2006**, *16*, 3906–3919.
21. Dahmen, U.; Hetherington, C.; Radmilovic, V.; Johnson, E.; Xiao, S.; Luo, C. Electron Microscopy Observations on the Role of Twinning in the Evolution of Microstructures. *Microsc. Microanal.* **2002**, *8*, 247–256.
22. Hofmeister, H. Fivefold Twinned Nanoparticles. In *Handbook of Nanotechnology*; Naiwa, H., Ed.; American Scientific Publishers: San Diego, CA, 2004.
23. de Wit, R. Partial Disclinations. *J. Phys. C: Solid State Phys.* **1972**, *5*, 529–534.
24. Stadelmann, P. A. EMS—A Software Package for Electron Diffraction Analysis and HREM Image Simulation in Materials Science. *Ultramicroscopy* **1987**, *21*, 131–146.
25. van Huis, M. A.; Kunneman, L. T.; Overgaag, K.; Xu, Q.; Pandraud, G.; Zandbergen, H. W.; Vanmaekelbergh, D. Low-Temperature Nanocrystal Unification through Rotations and Relaxations Probed by *In Situ* Transmission Electron Microscopy. *Nano Lett.* **2008**, *8*, 3959–3963.